DOMAIN GROWTH LAW VIOLATIONS IN A COMPRESSIBLE 2D ISING MODEL

by

Matthew Robert Wright

A senior thesis submitted to the faculty of

Brigham Young University

in partial fulfillment of the requirements for the degree of

Bachelor of Science

Department of Physics and Astronomy

Brigham Young University

August 2007

BRIGHAM YOUNG UNIVERSITY

DEPARTMENT APPROVAL

of a senior thesis submitted by

Matthew Robert Wright

This thesis has been reviewed by the research advisor, research coordinator, and department chair and has been found to be satisfactory.

Date	Gus Hart, Advisor
Date	Eric Hintz, Research Coordinator
Date	Ross L. Spencer, Chair

ABSTRACT

DOMAIN GROWTH LAW VIOLATIONS IN A COMPRESSIBLE 2D ISING MODEL

Matthew Robert Wright

Department of Physics and Astronomy

Bachelor of Science

Phase separation is the process when a homogeneous mixture separates into two (or more) different phases. This process is found in systems such as binary alloys where it affects properties such as hardness. We study domain growth tendencies of a phase-separating binary alloy using a two-dimensional, spin-exchange Ising model. The model obeys the asymptotic domain growth law (of the form $R \propto t^{\frac{1}{3}}$, where R is the size of the domain and t is time) when the model is allowed to respond to compressive forces. However, when compressibility and different atomic sizes are introduced into the model, the domain growth law is violated and we observe qualitatively different domain growth patterns. The exponent in the growth law is found to be less than 0.27 for the simulations with different atomic sizes. This violation indicates a lack in the current theory of domain growth and suggests fundamental properties of precipitate hardening processes in alloys are still not understood.

ACKNOWLEDGMENTS

I would like to thank Gus Hart for all the help he gave me, especially with the idea and theory of the matter and with help throughout. I would also like to thank my wife, Sherry, for putting up with all the long nights I worked on this.

Contents

List of Figures

Chapter 1

Introduction

Phase separation is the process when a homogeneous mixture separates into two (or more) different phases. This process is found in systems such as binary alloys where it affects properties such as hardness. One example of phase separation occures in duralumin, an alloy of aluminum with 4% copper. With the addition of copper, the aluminum becomes much harder and has greater tensile strength than pure aluminum. Small amounts other additives may be included to further strengthen the alloy or to produce other results. There are two stable phases in duralumin (when containing just aluminum and copper) at room temperature: the pure aluminum phase and the $CuAl_2$ phase. At a sufficiently high temperature, the $CuAl_2$ phase dissolves and the copper disperses evenly throughout the alloy. If the mixture is heated to this temperature and then slowly cooled, large grains of the $CuAl_2$ phase will form. These large grains do not strengthen the aluminum very much. However, heating the alloy then quickly cooling it facilitates the formation of many small grains of $CuAl_2$ which strengthens the alloy significantly.

Immediately after the rapid cooling, small, isolated particles of the $CuAl_2$ phase form throughout the material. To form small grains of the $CuAl_2$ phase, the alloy

is put through a process called "age-hardening" or "aging." After cooling the alloy, its temperature is increased, but not to the point where the $CuAl_2$ phase dissolves again. This temperature is held for a while. During this aging process, the particles of the $CuAl_2$ phase come together to form grains. If this temperature is held for too long, these grains would become very large and our alloy would not be as strong. However, if aging is controlled properly, many small grains of the $CuAl_2$ phase will form. These small grains of the $CuAl_2$ phase dispersed throughout the alloy help reduce dislocations. This results in the metal being harder.

In 1961, I. M. Lifshitz and V. V. Slyozov published a paper that calculated equations governing phase separation in a dilute solution [2] such as duralumin. They determined that the radius of the grains of the less predominant material grows asymptotically in proportion to $t^{\frac{1}{3}}$, where t is time and $\frac{1}{3}$ is the growth exponent. In early papers, simulations attempting to substantiate this grain growth law showed that it was not valid, but that the growth exponent should be less than 0.25 [16–18]. However, these results were erroneous due to an insufficient number of particles in the simulation and/or not running the simulation long enough to reach the asymptotic tendencies. In 1986, David A. Huse generalized Lifshitz's results to show that growth of domains in *equal fractions* of two substances follow the same growth law ($\propto t^{\frac{1}{3}}$) [3]. Huse's derivation applied to two-dimensional models as well as three-dimensional models. Soon after Huse's paper, simulations showed the domain growth law was valid [4].

Recently, however, S. J. Mitchell and D. P. Landau published a paper where they found the domain growth law was violated in size-mismatched systems. Their model was a two-dimensional, spin-exchange Ising model with an equal number of the two atoms and continuous particle positions and the two atomic species had different sizes [1]. Their simulations exhibited asymptotic domain growth, so this

inconsistency indicates a lack of understanding of domain growth. This paper explains and replicates their model. Then, we convert the model to a hexagonal lattice. We find that the hexagonal lattice model also violates the domain growth law when the atoms have continuous particle positions and the two atomic species had different sizes.

Chapter 2

Background

2.1 Ising Model

As mentioned in Chapter 1, Mitchell and Landau used a two-dimensional, spin-exchange Ising model with an equal ratio of two atoms to simulate domain growth. The Ising model is a simplified model of a ferromagnet (or paramagnet). It is described in Ernst Ising's doctoral thesis in 1924 [5]. Ising proposed that a magnet can be though of as a chain of dipoles. These dipoles could represent individual iron atoms. He assumes that each dipole only had magnetic interactions with each of its nearest neighbors. That is, he ignores long-range magnetic interactions. He further assumes that all the individual dipoles had one axis of magnetization so these dipoles could only have two possible orientations along this axis: parallel (up) or antiparallel (down).

Each dipole (except for the end dipoles) has two nearest neighbores in Ising's model. We call J the interaction energy of two neighboring dipoles oriented parallel to each other. Then, if two neighboring dipoles have opposite orientations, their interaction energy would be $-J$. If $J < 0$, the Ising model simulates ferromagnetism.

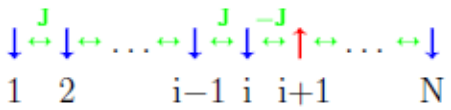

Figure 2.1 A possible configuration of a chain of dipoles in the 1D Ising Model. The dipoles oriented down are shaded blue and the dipoles oriented up are shaded red for convenience. The green arrows represent the interactions between neighboring dipoles. The energy of some interactions ($\pm J$) is shown above the interaction.

This is because the state with lowest energy is when all the dipoles are aligned, as in a ferromagnet. If $J > 0$, the Ising model simulates paramagnetism, since each dipole prefers to be anti-aligned with its neighbors. A pictorial representation of Ising's model is shown in Figure 2.1. Here, colored arrows indicating the direction of orientation represent individual dipoles. The interactions between dipoles and their energies are shown in green. For example, since dipoles 1 and 2 are both oriented down, their interaction energy is J. Since dipole j is oriented down and dipole $j-1$ is oriented up, their interaction energy is $-J$.

The Ising model has applications beyond the realm of magnetization. By replacing the dipoles with the occupation of sites, the Ising model represents the *lattice gas* model of a fluid [7]. The Ising model can also describe the ordering or unmixing of binary alloys (AB), as with Mitchell's and Landau's paper. This is accomplished by assuming the two possible orientations of dipoles are actually two different chemical species (A and B) and requiring that the number of each species is fixed. Then, instead of just allowing dipoles to flip as in the magnetic model, we can only consider the exchange of neighboring atoms. This method of exchanging neighbors in an Ising model is called spin-exchange. If $J < 0$ in this binary alloy model, we model phase separation. If $J > 0$, we model ordering, where the elements evenly mix.

One reason Ising proposed his model was to study the phase transition in a magnet.

A phase transition is the process by which a system undergoes a discontinuous change of its properties, such as a magnet abruptly changing from a magnetized state to an unmagnetized state at a certain temperature. The temperature where this phase transition occurs is called the Curie temperature T_{C}. In his 1924 doctoral thesis, Ernst Ising solved the one-dimensional Ising model and shows that it does not have a phase transition, but smoothly changes from the magnetized state to the unmagnetized state with increasing temperature [5]. Later, in 1943, Lars Onsager extended the Ising model into two dimensions and solved it, showing that it does exhibit a phase transition [6]. The Curie temperature was found to be the solution of the equation:

$$\sinh^2\left(\frac{2J}{k_{\mathrm{B}}T_{\mathrm{C}}}\right) = 1$$

with J being the interaction energy (as above) and k_{B} the Boltzmann constant. Thus, in units of $\frac{J}{k_{\mathrm{B}}}$, $T_{\mathrm{C}} \approx 2.27$. To obtain this result, Onsager assumed the system had periodic boundary conditions. Thus every dipole, even on the edge of the simulation, has four nearest-neighbors. A pictorial representation with only a few interactions depicted is shown in Figure 2.2. The analytical solution to any three-dimensional Ising model has eluded scientists thus far.

2.2 Monte Carlo method

Rather than analytically solving the Ising model, Mitchell and Landau use the Monte Carlo method to perform their simulations. The Monte Carlo method is a computational, stochastic method for solving problems. Its name was proposed by early implementers of the method, notably N. Metropolis and S. Ulam [10]. Since the Monte Carlo method follows similar rules to the rules of chance found in gambling, some claim this method was named after Monte Carlo, the city in Monaco famous for gambling.

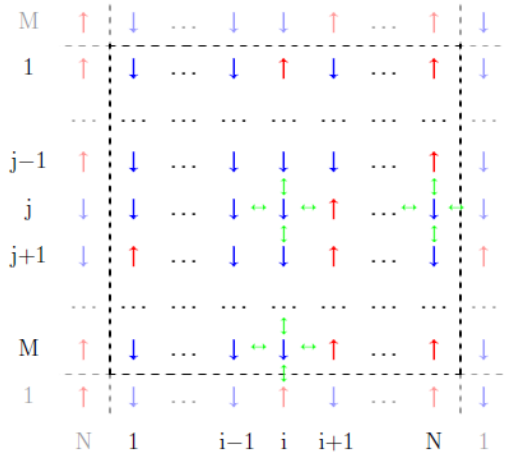

Figure 2.2 A possible configuration of dipoles of a 2D Ising Model. The dipoles oriented down are shaded blue and the dipoles oriented up are shaded red for convenience. The green arrows represent a selection of the interactions between neighboring dipoles. This model employs periodic boundary conditions, which is indicated by the "repeated" (faded) dipoles all around.

The Monte Carlo method uses (pseudo-)random numbers to approximate solutions to problems through stochastic simulation. Usually, these problems are difficult or impossible to solve using other methods. These random numbers must follow a specified distribution that depends on the problem being studied. This distribution is usually obtained by generating random numbers within a uniform distribution and then applying a function to these numbers to bring them to the appropriate distribution. For our simulations, a uniform distribution is sufficient.

For the most common application of the Monte Carlo method, Monte Carlo integration, the random numbers are used as "test" points for the integration. An example of Monte Carlo integration is presented as the remainder of this section. For deterministic simulations, such as those that follow the Metropolis Algorithm, the random numbers advance the simulation to another state. See Section 2.3 for an example of the Metropolis Algorithm.

As an example of the Monte Carlo method, we consider Monte Carlo Integration.

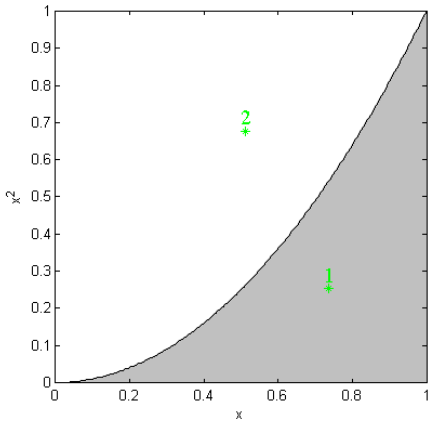

Figure 2.3 Plot of x^2 with two Monte Carlo "guesses." The shaded part of the graph is the area we are trying to find. Point one is a "hit" while point two is not.

Normal numerical integration involves dividing the domain into many small regions, then summing the value of the function over all the regions. Where this method works quite well with some integrals, it works poorly for integrals involving multiple degrees of freedom. For an integral with 100 degrees of freedom, dividing each dimension into only 10 regions involves 10^{100} evaluations! This is not computationally feasible. The Monte Carlo method of integration suits such complicated integrals much better.

To demonstrate Monte Carlo integration, we calculate the area under the curve $f(x) = x^2$ on the interval $x \in [0, 1]$ (see Figure 2.3). To do this, we generate two random numbers, x and y, each between 0 and 1. If the point (x, y) lies in the shaded area of the graph, the point is a "hit." This can be determined by checking if $y \leq x^2$. We generate many points, counting how many "hits" we get. Then, it is easy to show that

$$\frac{\#\text{ of "hits"}}{\text{total }\#\text{ of points}} \approx \frac{\text{area under } x^2}{\text{area of the } 1 \times 1 \text{ square}} = \text{Area}.$$

Using this method on a computer for 10,000 points yields Area ≈ 0.3282. This problem was somewhat trivial, for we know that the solution to this problem is

$$\text{Area} = \int_0^1 x^2\,dx = \frac{1}{3}.$$

We see how using the Monte Carlo method of integration gave an approximate solution to the problem. Where other methods of integration work well in low-dimensional integration, Monte Carlo integration is much more efficient as the dimensionality of the problem increases.

2.3 Metropolis Algorithm

The Metropolis algorithm describes a computational Monte Carlo method of determining the probable states of a (thermodynamic) system. It was originally proposed by Nicholas Metropolis, et al. in 1953 [9]. The algorithm is as follows:

1. Start the system in any state, with fixed temperature T.

2. Change the system into a "nearby" state. This might be accomplished by exchanging one pair of neighboring atoms or moving one particle, as in our models.

3. This change is tested using the Metropolis Acceptance rate as follows:

   If the energy of the "new" state is lower than the energy of the former state, keep the change—that is, use the new state for the next stage of the algorithm.

   If the energy of the "new" state is greater than the energy of the former state, determin whether to keep the change dependent on temperature with the following procedure:

   - Generate a random number ρ in a uniform distribution between 0 and 1.

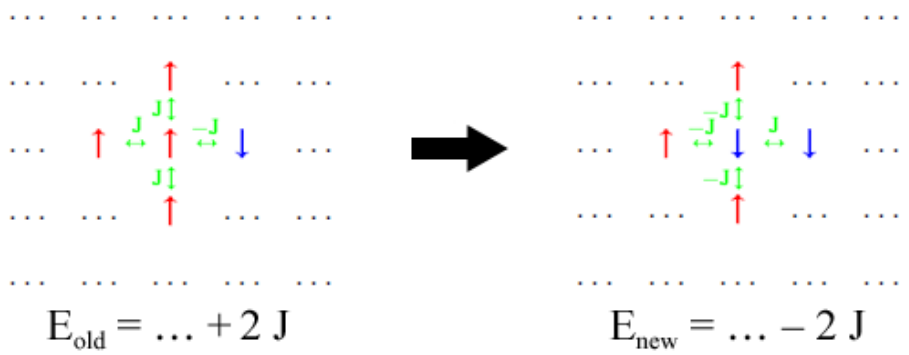

Figure 2.4 The Metropolis Algorithm applied to a 2D Ising model. The dipoles oriented down are shaded blue and the dipoles oriented up are shaded red for convenience. The green arrows represent the interactions between neighboring dipoles. The central dipole is flipped to change the system to a "nearby state."

- Calculate the the Boltzmann factor: $e^{\frac{-(E_{\text{new}}-E_{\text{old}})}{k_B T}}$.
- If $\rho \leq e^{\frac{-(E_{\text{new}}-E_{\text{old}})}{k_B T}}$ keep the change.
- If $\rho > e^{\frac{-(E_{\text{new}}-E_{\text{old}})}{k_B T}}$ reject the change—that is, use the old state for the next stage of the algorithm.

4. Repeat steps 2–3 for many changes.

How many times to repeat steps 2–3 and what data to record depends on the system being studied. With our models, we repeat steps 2–3 $512^2 \times 10^6$ times and record some internal data about every $512^2 \times 10^3$ repetitions (see below).

As an example of the Metropolis Algorithm, we consider a two dimensional ferromagnetic Ising model. Step 1: We begin with a random configuration of dipoles and set $T = 0.6\frac{|J|}{k_B}$. Let part of the model look like that shown on the left in Figure 2.4. Step 2: We change our system to a "nearby" state by flipping the central dipole in the figure to the configuration shown on the right of Figure 2.4. Step 3: Since $J < 0$ (ferromagnetic), we see that $E_{\text{new}} > E_{\text{old}}$. So, we generate a random number ρ

between 0 and 1. We will use the random number $\rho = 0.582$. We now consider the Boltzmann factor:

$$e^{\frac{-(E_{\text{new}}-E_{\text{old}})}{k_B T}} = e^{\frac{-(-4J)}{0.6|J|}} = e^{-\frac{20}{3}} \approx 0.00127.$$

Since $0.582 > 0.00127$, we reject change, and return our system to the previous state, that is, flip the central dipole back to its original orientation (the configuration shown on the left of Figure 2.4). Step 4: To continue the Metropolis algorithm, we select another dipole (perhaps even the same one) and try this same procedure (of flipping the dipole) again. Over multiple repetitions of steps 2–3, our system evolves, simulating thermodynamic evolution of a magnet.

2.4 Lennard-Jones Potential

To better simulate atoms in a real system, Mitchell and Landau allow the particles to move. They employ a Lennard-Jones potential to model how each atom interacts with neighboring atoms to maintain a crystal structure. The Lennard-Jones potential (see Figure 2.5) is an approximation of the interaction potential between two uncharged molecules or atoms. It was proposed by John Lennard-Jones in his paper published in 1931 [11]. It can be written either

$$V(r) = 4\epsilon \left[\left(\frac{\sigma}{r}\right)^{12} - \left(\frac{\sigma}{r}\right)^{6} \right]$$

or

$$V(r) = \epsilon \left[\left(\frac{r_0}{r}\right)^{12} - 2\left(\frac{r_0}{r}\right)^{6} \right]$$

where r is the distance between particles, ϵ is the depth of the potential well, σ is the (finite) distance where the potential energy is zero, and $r_0 = 2^{1/6}\sigma$ is the distance where the inter-particle force is zero (the minimum of the potential well).

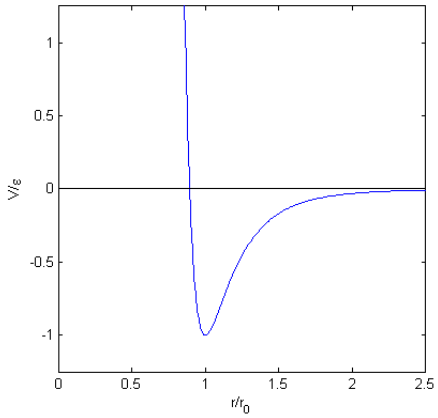

Figure 2.5 The Lennard-Jones Potential. The x-axis is in units of r_0. The y-axis is in units of ϵ.

The first term in the Lennard-Jones potential ($\propto r^{-12}$) models the repulsive force arising from the Pauli Exclusion principle. This repulsion is caused by the wave functions of each atom overlapping and repelling each other. The theoretical form of this term is actually proportional to e^{-ar}, but is chosen to be proportional to r^{-12} for ease of calculation ($r^{-12} = (r^{-6})^2$). The second term ($\propto r^{-6}$) is attractive and arises from a dispersion interaction which is the cause of *van der Waals* forces. As electron density shifts (due to random fluctuations) to one side of an atom, a momentary dipole is formed. This dipole induces a dipole in the other atom. These momentary dipoles attract each other, causing the dispersion interaction.

2.5 Correlation Function

As we are checking the validity of the domain growth law, it seems appropriate to define the size of a domain. For small amounts of one of species, Lifshitz and Slyozov define the size of the grains of these atoms as the radius of the grains [2]. However, when considering equal numbers of each atom, the two species form large domains. One domain can extend through the entire substance. To measure the size of the

domains, Huse uses the first zero crossing of the correlation function, which we call the correlation length [3].

For the ferromagnetic Ising model, nearest-neighbor dipoles prefer to have the same orientation. That is, they are correlated with each other. Since nearest-neighbor dipoles prefer to be oriented the same way, next nearest-neighbors also prefer to have the same orientation. The correlation function is a quantitative measure of this clustering of like particles. The correlation function for the Ising model can be written

$$C(r) = \langle s_i s_j \rangle - \langle s_i \rangle^2$$

where s_i and s_j are numeric values of individual dipoles (1 = up and -1 = down) with s_i and s_j being separated by the distance r. For a typical correlation function, at small distances (r), the correlation function is above zero, that is the atoms are correlated. As r increases, the correlation function decreases, eventually crossing zero into negative numbers. That is, as we go farther away from our starting dipole, the dipoles aren't as likely to be aligned the same orientation.

To calculate the correlation function, we begin by choosing one specific dipole s_i. We consider the dipole oriented down represented in the middle of Figure 2.6**a**. At the distance $r = 1$ (in terms of the atomic spacing) from the central dipole, there are four dipoles: above, below, right and left, each of which we represent by s_j. Each of these dipoles are oriented down. Thus, for each dipole, $s_i s_j = (-1) \times (-1) = 1$. The average value is therefore $\langle s_i s_j \rangle = 1$. When we go the distance $r = \sqrt{1^2 + 1^2} = \sqrt{2}$ away, we again find four dipoles. Three are oriented down, but one is oriented up. Then, the average value is $\langle s_i s_j \rangle = \frac{1+1+1+-1}{4} = 0.5$. We repeat this process of selecting a distance and determining $\langle s_i s_j \rangle$ for all distances where there are dipoles. For this particular system state, this part of the correlation function (pertaining just to this s_i) is graphed in Figure 2.6**b**. We see that the tendency to be correlated tends to

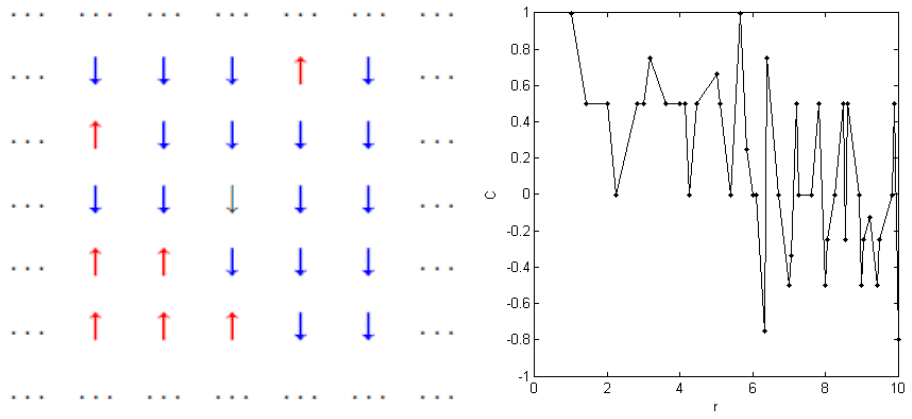

(a) **(b)**

Figure 2.6 **(a)** Part of a configuration of dipoles of a 2D Ising Model. The dipoles oriented down are shaded blue and the dipoles oriented up are shaded red for convenience. The dipole in the middle is used as reference for the description of the correlation function. **(b)** The part of the correlation function added by the central dipole in **(a)**. As this function is averaged over many atoms, the function will become smoother. The average magnetization for the entire system (not shown) is zero.

decrease over distance. We average each of these functions over every dipole s_i. We then average each of the resulting functions over many possible states of the system to obtain the $\langle s_i s_j \rangle$ part of the correlation function. For the $\langle s_i \rangle^2$ part of the correlation function, we sum up the numerical value of each dipole in the system and divide that by the total number of dipoles in the system. We average this over many possible states also. The correlation function subtracts the $\langle s_i \rangle^2$ term to remove the effect of any overall magnetization. The "correlation function" produced over just one state is shown in Figure 2.7**a**.

Also included in Figure 2.7**a** are some variations of the correlation function. Instead of calculating the full correlation function, we instead only consider dipoles lying along one direction. Thus, if going along the $(0, 1)$ or $(1, 0)$ direction, our correlation function only has a value at integer rs. So also, if going along $(1, 1)$ or $(1, -1)$, the

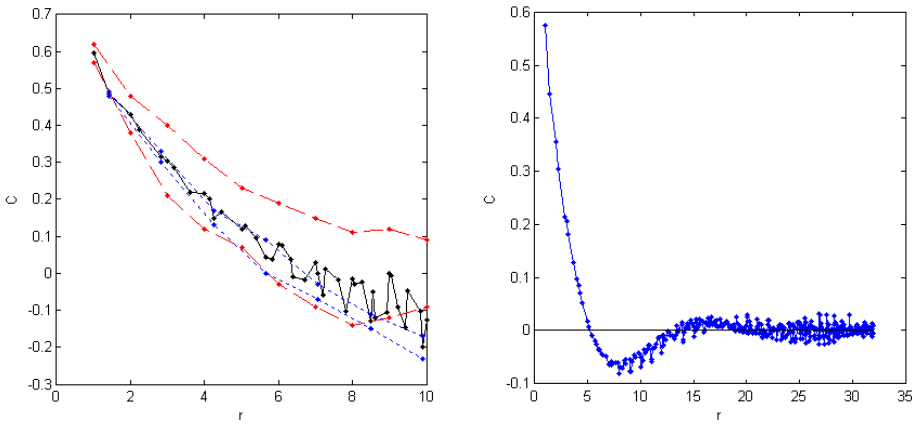

(a) **(b)**

Figure 2.7 A plot of various correlation functions of a 2D Ising model. The correlation functions are averaged over every dipole in the system (but not averaged over "time"). **(a)** The black line is the full correlation function. The red dashed lines are correlation functions along the cardinal directions averaged over every dipole. The blue dotted lines are correlation functions along the diagonal directions ((1,1) and (1,-1)) averaged over every dipole. **(b)** A plot of the correlation function of a spin-exchange 2D Ising model. One can approximately see how the correlation function intersects zero in an oscillatory nature.

correlation function only has values at integer multiples of $\sqrt{2}$. As shown in Figure 2.7**a**, these functions somewhat follow the full correlation function.

Figure 2.7**b** shows a correlation function for a spin-exchange Ising model with equal fractions of each particle. We see how the correlation function drops below zero then oscillates. Like Huse, we define the correlation length as the first zero of the correlation function. The correlation length is calculated by fitting data near the intersection point to a quadratic equation and determining the x-intercept of this fit. A quadratic fit is chosen as it gives the closest fit of all fits up to a polynomial of order $\sim$7 and is computationally easy.

Chapter 3

Methods

We study the asymptotic domain growth of phase separation in a binary alloy. To do this, we perform six sets of Monte Carlo simulations of a two-dimensional, spin-exchange Ising model with an equal ratio of the two species. We set A atoms to be "dipoles" oriented down and B atoms to be "dipoles" oriented up. We use the Metropolis algorithm [9] to evolve our system as we study the formation of large domains. We define a Monte Carlo move (MCM) to be one repetition of steps 2–3 in the Metropolis algorithm. Each simulation uses periodic boundary conditions, which can be thought of as the simulation modeling one cell in a crystal.

We perform three of our models on a square lattice. The other three models use a hexagonal lattice. Two of our models (one square and one hexagonal) are normal, two-dimensional, spin-exchange Ising models. We call these models the "rigid" models. Our Hamiltonian for these models is given by that of the standard Ising Model:

$$H = \sum_{s_i, s_j} J_{\mathrm{R}} s_i s_j \tag{3.1}$$

with $J_{\mathrm{R}} = -1$. (If we set $J_{\mathrm{R}} = +1$, then we have an ordering model, rather than a phase-separating model.) The sum is over each pair of nearest neighbor atoms (s_i and

s_j). The product $s_i s_j$ is the product of the numerical value of each atom (A = −1, B = +1). One MCM consists of testing a randomly chosen nearest neighbor exchange.

The other models are also two-dimensional, spin-exchange Ising models, but we allow our atoms to have continuous positions, with initial positions on lattice. This allows the atoms in the system to respond to compressive forces. Thus, we call the models that use this method compressible. To account for this compressibility, we use a different Hamiltonian. We use a standard Lennard-Jones potential and a bond-angle stiffness term:

$$H = \sum_{s_i,s_j} J_{ij} \left[\left(\frac{\ell_{ij}}{r_{ij}} \right)^{12} - 2 \left(\frac{\ell_{ij}}{r_{ij}} \right)^{6} \right] + \sum_{s_i} \sum_{s_j,s_k} J_\theta \cos^2 (\eta \theta_{jik}) \tag{3.2}$$

We define J_{ij} to be the depth of the potential well of the Lennard-Jones potential. J_{ij} can also be interpreted as the tendency for the atoms to stay the distance ℓ_{ij} apart from each other. We define J_θ to be the bond-angle stiffness. As the value of J_θ increases, the bond angle deviates less from the desired angle (see below). The Lennard-Jones potential tends to keep the atoms at their preferred spacing. If including just the Lennard-Jones potential for the special case where $\ell_{ij} = 1$, the atoms would eventually try to form a hexagonal lattice because that is the most efficient way of placing atoms that are equally spaced in two dimensions. To prevent our atoms from forming this hexagonal lattice, we include the bond-angle stiffness term. By making the energy cost of changing the angle high (J_θ is comparable to J_{ij}), the atoms tend to maintain the desired lattice. For notation, if s_i is an atom of type B, and if s_j is an atom of type A, then $r_{ij} = r_{\mathrm{BA}}$, $\ell_{ij} = \ell_{\mathrm{BA}}$, etc.

For the first (Lennard-Jones) component of the Hamiltonian, the sum runs over each nearest-neighbor pair (s_i and s_j). r_{ij} is the distance between each of these nearest-neighbor pairs. We define ℓ_{ij} to be the preferred distance between each type pair. (ℓ_{ij} is the distance where the Lennard-Jones potential is at a minimum.)

For the second (bond angle) component of the Hamiltonian, the first sum runs over each atom (s_i). For each atom, we sum over each pair of "closest" nearest-neighbor atoms (s_j and s_k). Not all possible pairs of nearest-neighbors are included in the second sum, only those which are "next" to each other. For example, if the atoms are on a square lattice, there are only four pairs (not six), each $\sim$90° apart. For a hexagonal lattice, there are only six pairs, each $\sim$60° apart. The angle from s_j to s_i to s_k is defined as θ_{jik}. To account for the difference in bond angle between different lattices, we include a bond-angle correction factor η inside the cos term. If $\eta = 1$, then the atoms will form a square lattice. If $\eta = \frac{3}{2}$, then the atoms will form a hexagonal lattice.

If we set $J_{\mathrm{AA}} = J_{\mathrm{BB}} = \infty$, $J_{\mathrm{AB}} = J_{\mathrm{BA}} = J_{\mathrm{AA}} - 2$, $\ell_{ij} = 1$, and start the atoms on a square lattice, our model reduces to the square, "rigid" model. So also if we set $J_\theta = \infty$, $\eta = 1$ and start the atoms on a square lattice, we reduce to the square, "rigid" model. We obtain similar results for the hexagonal lattice with $\eta = \frac{3}{2}$. Thus, by setting $J_{\mathrm{AB}} = J_{\mathrm{BA}} = J_{\mathrm{AA}} - 2$, $\ell_{ij} = 1$ and $\eta = 1$, we can compare our compressible model to the standard two-dimensional, spin-exchange Ising model. Similarly, if we set $J_{\mathrm{AB}} = J_{\mathrm{BA}} = J_{\mathrm{AA}} - 2$, $\ell_{ij} = 1$ and $\eta = \frac{3}{2}$, the compressible, hexagonal models compare with the hexagonal "rigid" model. In particular, following these requirements keeps the Curie temperature of the compressible models close to that of the "rigid" models [19].

For each MCM in the compressible models, we test either a randomly chosen nearest neighbor exchange or a small random move of a randomly chosen atom. If moving an atom, one of the cardinal directions is chosen and the atom is displaced a small, random amount. We test this displacement using the standard Metropolis acceptance rate.

Chapter 4

The Simulation

We perform six sets of Monte Carlo simulations modeling binary alloys with a two-dimensional, spin-exchange Ising model with an equal ratio of the two species. We perform half of our simulations on a square lattice, with the other half on a hexagonal lattice. For each lattice, we perform three sets of simulations: "rigid", "matched", and "mismatched." The "rigid" models run with the atoms on lattice, as described above. The "matched" simulations are compressible, as described above, with equal preferred inter-particle distances ($\ell_{\mathrm{AA}} = \ell_{\mathrm{BB}}$). The "mismatched" simulations are also compressible, but the A and B atoms have different preferred inter-particle distances ($\ell_{\mathrm{AA}} \neq \ell_{\mathrm{BB}}$, see below).

We use a lattice of 512×512 atoms in our simulations. We define one Monte-Carlo Sweep (MCS) as 512^2 Monte Carlo moves. With our lattice size, we did not observe (qualitatively) finite size effects below 10^6 MCS. We found that our models began to exhibit asymptotic growth tendencies before 10^5 MCS. So, we allow each simulation to run for 10^6 MCS to observe asymptotic growth while obtaining a sufficient amount of data.

For the compressible simulations, we set $J_{\mathrm{AA}} = J_{\mathrm{BB}} = 30$, $J_{\mathrm{AB}} = J_{\mathrm{BA}} = J_{\mathrm{AA}} - 2 =$

28, and $J_\theta = 50$. These constants are chosen to allow the models to behave similar to the "rigid" model (see above). The specific values are chosen to compare to the work of Mitchell and Landau [1]. As appropriate, we set $\eta = 1$ for the square lattice and $\eta = \frac{3}{2}$ for the hexagonal lattice. As expected, for the hexagonal lattice, some significant differences in the nature of the model are found, but the behavior of domain growth is the same.

For the "matched" models, $\ell_{ij} = 1$ for all combinations of i and j. For the "mismatched" models, we put $\ell_{\mathrm{AA}} = 1.02$, $\ell_{\mathrm{BB}} = 0.98$, and $\ell_{\mathrm{AB}} = \ell_{\mathrm{BA}} = 1$. The difference in preferred inter-particle distances is chosen to represent the phase separation in SiGe [13–15] as also to compare our results with the work of Mitchell and Landau [1]. The small variation of ℓ in the "mismatched" models does not seem to change the Curie temperature significantly [19], though it does change some aspects of the model as will be shown.

For each of the compressible models, after each MCS we attempt a small, random total volume adjustment, with the same Metropolis acceptance rate. This volume adjustment requires terms not mentioned in the previous Hamiltonian. The formula for the effective Hamiltonian dependent on volume is:

$$H_V = PV - Nk_{\mathrm{B}}T\ln(V). \tag{4.1}$$

We set our pressure (P) equal to zero in each simulation.

For each simulation, we start out with a random configuration of atoms placed on lattice with an equal ratio of the two species. Then, we equilibrate the simulation at $k_{\mathrm{B}}T = 7$ for the square lattice and $k_{\mathrm{B}}T = 14$ for the hexagonal lattice. After equilibrating, we set the temperature to $k_{\mathrm{B}}T = 1.5$ for the square lattice and $k_{\mathrm{B}}T = 2.7$ for the hexagonal lattice for the remainder of the simulation. These values are selected so that the bulk of the simulation is performed at $T \approx \frac{2}{3}T_{\mathrm{C}}$ for the "rigid"

models, where T_C is the Curie temperature. Curie temperatures for square lattice models are $T_C \approx 2.25$ and the hexagonal lattice models have $T_C \approx 4.5$. (Units are in terms of J_R for the "rigid" models and $\frac{J_{AA}-J_{AB}}{2}$ for the other models.) Making the model compressible does not seem to change the Curie temperatures too significantly, though no accurate quantitative results could be produced [19].

To measure the rate of domain growth, we calculate the effective correlation length every 10^3 MCS or less. For ease of computation, we only compute the correlation function in the principle directions ($(0,1)$ and $(1,0)$ for the square lattice and $(0,1)$, $(\frac{1}{2},\frac{\sqrt{3}}{2})$ and $(-\frac{1}{2},\frac{\sqrt{3}}{2})$ for the hexagonal lattice) over one system state. We calculate a correlation length for each correlation function an average them over four single-system states. We generate these different states by running the simulation for one MCS between each calculation. As seen in Figure 2.7, the correlation lengths are not the same in the principle directions. To compensate for the difference in correlation lengths, the effective correlation length ξ is calculated by averaging the average correlation lengths over the primary directions. After running several simulations, the effective correlation lengthes are averaged over all the simulations in each specific model, then fit to the equation:

$$\xi = A + Bt^n \tag{4.2}$$

to extrapolate the growth exponent n. MatLab's fitter is used to calculate these fits. As expected, the domain growth of each model does not follow logarithmic growth or other growth, but follows t^n very well.

Chapter 5

Results

Qualitatively, all of the models behaved similarly: the width of the domains grow over time. Some snapshots of each model at times (in terms of MCS) 10^4, 10^5, 10^6 are shown in Figure 5.1. The domains grow over time, narrower domains diffusing into and connecting with the larger domains. The diagonal stripe domain growth in the square, "mismatched" simulation is interesting, but not uncommon [12]. The grain creation in the hexagonal, "mismatched" simulation is also interesting, but understandable. As the smaller atoms come together, they tend to take up less space than the larger atoms. Then, from a spatial perspective, the two substances occupy a different ratio of the whole, with the smaller atoms taking up $<50\%$. Thus, the smaller atoms form grains within the "substrate" of the larger atoms. Why the hexagonal lattice forms grains while the square lattice forms diagonal stripes is believed to be an effect of the choice of J_{ij} and J_θ, though no attempt to substantiate this claim was made. Orlikowski, et al. performed many simulations where they obtained different growth patterns for different stresses [12]. I believe the two effects are related.

As mentioned above, the method used to calculate the size of the domains is the effective correlation length. A plot of the effective correlation length for one of the

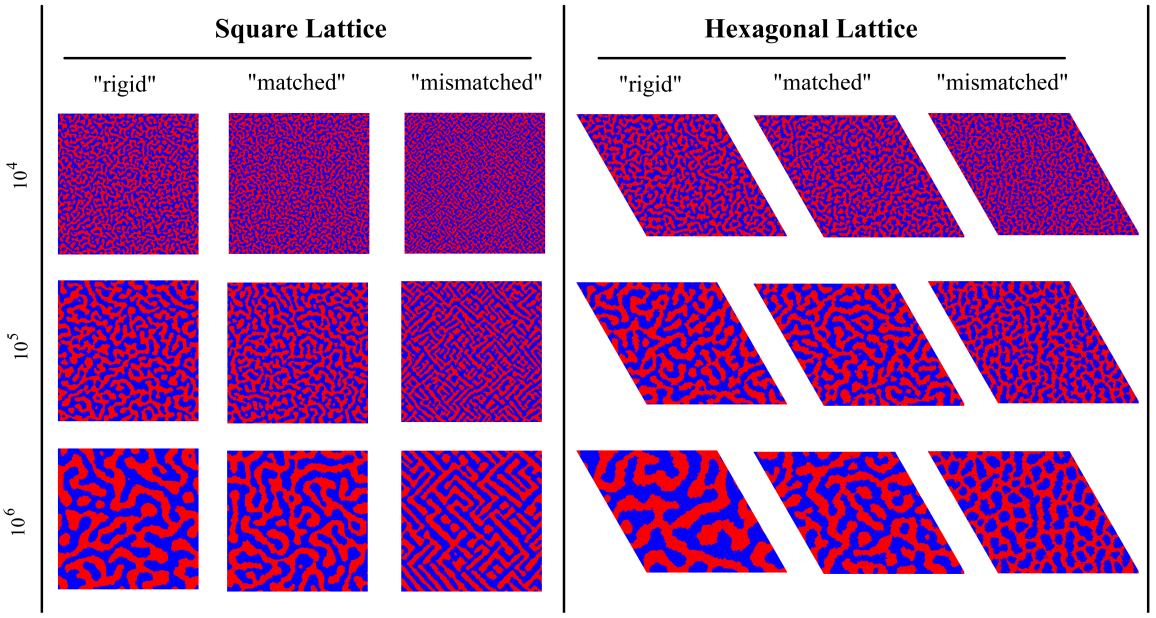

Figure 5.1 Snapshots at different times (MCS) for each model. $N = 512^2$. A atoms are represented by blue points, and B atoms are represented by red points. Each model was run at $k_{\mathrm{B}}T = 1.5$ for the square lattice and $k_{\mathrm{B}}T = 2.7$ for the hexagonal lattice.

"rigid" simulations on a square lattice is shown in Figure 5.2. The x-axis is time in terms of MCS. The y-axis is the effective correlation length ξ. This particular set of data follows the domain growth law very well, with $n = 0.332$. Also on this plot is the curve fit to this data. Shown in Figure 5.2b is a log-log plot of the same data. Comparing the average over the cardinal directions with the best fit, we can see the data closely follows the $n = \frac{1}{3}$ law. We can also see how the primary directions fluctuate, while the average remains mostly steady. It is common that at approximately 10^5 MCS, the separation of the primary directions becomes larger. This trend (of the primary directions separating at $\sim 10^5$ MCS) is observed in each model. It is believed that this is due to some spontaneous symmetry breaking at this point in the simulation. Which direction domain growth prefer is random and can even change later in the simulation. No discussion of the cause of this effect is

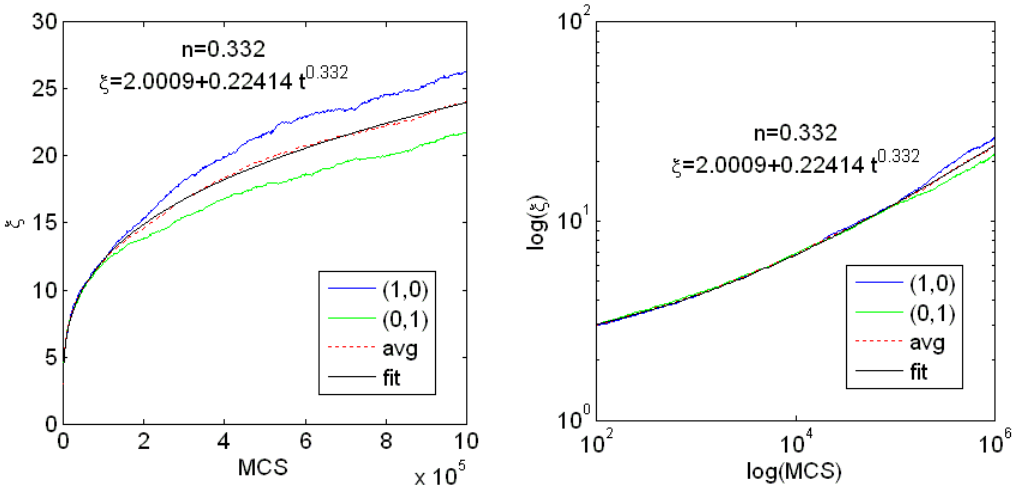

(a) (b)

Figure 5.2 Growth plot of a rigid simulation. The axis are MCS and ξ. Plotted are ξ in each of the cardinal directions, the average of these two, and data fit to the average. The run temperature was $k_{\mathrm{B}}T = 1.5$.

presented in this paper.

To determine the growth exponent for the data, we average all the effective correlation lengths over the number of simulations performed for each model. We then fit the data to Equation 4.2 for $t > 10^4$ MCS. Selections of these data are plotted in Figure 5.3. Also included in Figure 5.3 are several lines which are the fit to the data. Figure 5.3a contains the data for each of the square models. Figure 5.3b contains the data for each of the hexagonal models. We see how close the data matches our fit for $t > 10^4$ MCS. The error bars for these calculations are smaller than the sizes of the symbols used.

From the fits shown in Figure 5.3, we found the following growth exponents:

Model	Square Lattices	Hexagonal Lattices
"rigid"	$n = 0.3340 \pm 0.0004$	$n = 0.3329 \pm 0.0008$
"matched"	$n = 0.3294 \pm 0.0002$	$n = 0.3156 \pm 0.0007$
"mismatched"	$n = 0.2347 \pm 0.0003$	$n = 0.2672 \pm 0.0010$

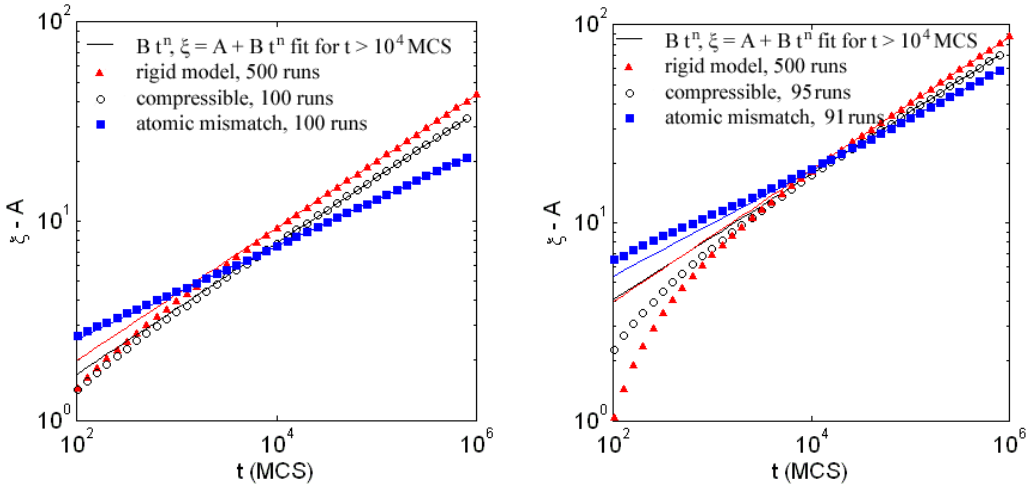

(a) **(b)**

Figure 5.3 $\xi - A$ averaged over multiple runs. A non-linear fit ($\xi = A + Bt^n$) was used to extrapolate A. The data for **(a)** came from the square lattice models. The data for **(b)** came from the hexagonal lattice models.

The calculated n for the "rigid" models are close to $n = \frac{1}{3}$. The ns found for the "matched" models are also close to $n = \frac{1}{3}$, though they are a little below the expected value. It is believed by the author that the smaller ns found for the "matched" models are an indication of an aspect not currently understood by the conventional theories. The term added by a correction should be small in comparison to $\frac{1}{3}$, but should be present in the asymptotic domain growth equation.

In both "mismatched" simulations, the calculated n is noticeably far from the expected $n = \frac{1}{3}$ growth law. These simulations are of sufficient precision and duration that it seems the asymptotic effects have been reached from the fitting to the data. This indicates a lack of complete understanding of the physics involved. I believe that this deviation is caused by the different preferred sizes affecting the nature of the surface of the domains because both Lifshitz and Huse assumed no abnormality on the surfaces of domains. The significant deviation from $n = \frac{1}{3}$ could indicate significant deviations in other equations governing domain and grain growth. Since

most real-world substances have different atomic sizes, these deviations suggests that we still do not understand the precipitate hardening process. With the development of a more accurate theory, we could potentially better control precipitate formation and create better alloys.

Bibliography

[1] S. J. Mitchell and D. P. Landau, "Phase Separation in a Compressible 2D Ising Model," Phys. Rev. Lett. **97,** 025701-1–4 (2006).

[2] I. M. Lifshitz and V. V. Slyozov, "The Kinetics of Precipitation from Supersaturated SolidSolutions," J. Phys. Chem. Solids **19,** 35–50 (1961).

[3] David A. Huse, "Corrections to late-stage behavior in spinodal decomposition: Lifshitz-Slyozov scaling and Monte-Carlo simulations," Phys. Rev. B **34,** 7845–7850 (1986)

[4] Jacques G. Amar, Francis E. Sullivan, Raymond D. Mountain, "Monte Carlo study of growth in the two-dimensional spin-exchange kinetic Ising model," Phys. Rev. B **37,** 196–208 (1988)

[5] E. Ising, "Beitrag zur Theorie des Ferro- und Paramagnetismus" (Thesis, Hamburg, 1924), (see: http://www.fh-augsburg.de/~harsch/germanica/Chronologie/20Jh/Ising/isi_intr.html), in German.

[6] Lars Onsager, "Crystal Statistics3: 1. A Two-Dimensional Model with and Order-Disorder Transition," Phys. Rev. **65,** 117–149 (1944)

[7] T. D. Lee, C. N. Yang, "Statistical Theory of Equations of State and Phase Transitions. II. Lattice Gas and Ising Model," Phys. Rev. **87,** 410–419 (1952)

[8] Daniel V. Schroeder, *A*n Introduction to Thermal Physics, 339–353 (Addison Wesley Longman, San Francisco, California, 2000).

[9] N. Metropolis, A. W. Rosenbluth, M. N. Rosenbluth, A. H. Teller, and E. Teller, "Equations of State Calculations by Fast Computing Machines," J. Chem. Phys., **21,** 1087–1092 (1953)

[10] N. Metropolis, S. Ulam, "The Monte Carlo Method," J. Am. Stat. Assoc., **44,** 335–341 (1949)

[11] J. E. Lennard-Jones, "Cohesion," Proc. Phys. Soc., **43,** 461–482 (1931)

[12] D. Orlikowski, C. Sagui, A. M. Somoza, and C. Roland, "Two- and three-dimensional simulations of the phase separation of elastically coherent binary alloys subject to external stresses," Phys. Rev. B **62,** 3160–3168 (2000).

[13] B. D*ü*nweg and D. P. Landau, "Phase diagram and critical behavior of the Si-Ge unmixing transition: A Monte Carlo study of a model with elastic degrees of freedom," Phys. Rev. B **48,** 14182–14197 (1993).

[14] M. Laradji, D. P. Landau, and B. D*ü*nweg, "Structural properties of $Si_{1-x}Ge_x$ alloys: A Monte Carlo simulation with the Stillinger-Weber potential," Phys. Rev. B **51,** 4894–4902 (1995). [ISI]

[15] F. Tavazza, D. P. Landau, and J. Adler, " Phase diagram and structural properties for a compressible Ising ferromagnet at constant volume,"Phys. Rev. B **70,** 184103-1–11 (2004).

[16] M. Rao, M. H Kalos, J. L. Lebowitz, and J. Marro, "Time evolution of a quenched binary alloy. III. Computer simulation of a two-dimensional model system," Phys. Rev. B **13,** 4328–4335 (1976).

[17] J. L. Lebowitz, J. Marro, and M. H. Kalos, "Dynamical scaling of structure function in quenched binary alloys," Acta Metall. **30,** 297–310 (1982).

[18] G. S. Crest, D. J. Srolovitz, "Structure and evolution of quenched Ising clusters," Phys. Rev. B **30,** 5150–?? (1984).

[19] There are no known articles proving these statements. These statements are found from qualitative observation of each model.